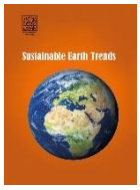
Shahid Beheshti University

Sustainable Earth Trends

Journal homepage: http://sustainearth.sbu.ac.ir



Spatial-temporal analysis of urban heat islands in shiraz using MODIS/GIS and providing urban planning solutions

Ali Heidari[a*], Ashraf Asadi[b]

[a] Department of Geography, Faculty of Literature and Humanities, Yasouj University, Yasouj, Iran
[b] Department of Geography, Payame Noor University, Tehran, Iran

ABSTRACT

Shiraz, recognized as the cultural capital of Iran, has increasingly faced the Surface Heat Island Urban (SHIU) phenomenon due to rapid urbanization and population growth. This study examines SHIU effects in Shiraz by analyzing Land Surface Temperature (LST) derived from MODIS satellite imagery (MOD11A2 and MCD12Q1 products) from 2000 to 2024, using GIS techniques to assess spatial thermal patterns and urban microclimate dynamics. The LinearFit function was applied to evaluate temporal trends in SHIU, while spatial variables-including building density, land cover, green space ratio, public green areas, population metrics, and construction activity-were analyzed across 11 urban zones. Findings revealed that daytime SHIU cores reached up to 32°C in the south, west, and parts of the north, while nighttime cores (13–14°C) expanded toward central and historic districts (Zone 8). The most significant nighttime LST increase (2–3°C) occurred in the northern and western zones (1, 4, 6, and 10), and to a lesser extent in the south (Zone 7), where substantial land cover changes and urban development were observed. These results underscore the critical need for climate-sensitive urban planning strategies. Integrating green infrastructure, regulating building density, and preserving open spaces can help mitigate SHIU effects and enhance urban resilience. The study provides actionable insights for policymakers, urban designers, and planners to promote sustainable development and improve thermal comfort in rapidly growing cities like Shiraz.

ARTICLE INFO

Keywords:
MODIS sensor images
Remote sensing
Shiraz
Surface Urban heat island
Urban planning

Article history:
Received: 16 April 2025
Accepted: 11 October 2025

*Corresponding author
E-mail address:
aheidari@yu.ac.ir
(A. Heidari)

Citation:
Heidari, A. & Asadi, A. (2026). Spatial-temporal analysis of urban heat islands in shiraz using MODIS/GIS and providing urban planning solutions, *Sustainable Earth Trends:* 6(4), (15-29).

DOI: 10.48308/set.2025.239529.1118

1. Introduction

With the rapid growth of urbanization, land use patterns and surface characteristics have undergone significant transformations, leading to changes in intra-urban microclimates. One of the most extensively studied phenomena in urban climatology is the Surface Urban Heat Island (SUHI) effect, a condition in which urban areas exhibit significantly higher temperatures compared to their surrounding rural zones. Understanding the causes and consequences of SUHI is essential for sustainable urban planning and climate adaptation. Key factors contributing to SUHI formation include: Land surface modification (The replacement of natural, permeable surfaces with impervious materials such as asphalt and concrete, which absorb solar radiation and release heat at night, Vegetation loss (The reduction of green spaces limits cooling through evapotranspiration and shading), Urban geometry, (Narrow streets and tall buildings trap heat and restrict airflow, leading to the “urban canyon” effect), Anthropogenic heat, (Transportation, industrial activities, and energy consumption inject additional heat into the urban atmosphere), Air pollution (Pollutants absorb and scatter solar radiation, altering the radiative balance and contributing to localized warming) (Imran et al., 2021; Vujovic et al., 2021). The SUHI effect typically intensifies during calm and clear nights when stored heat from urban surfaces is released into the atmosphere. Its intensity can range from

Copyright: © 2026 by the authors. Submitted for possible open access publication under the terms and conditions of the Creative Commons Attribution (CC BY). license (https://creativecommons.org/licenses/by/4.0/).

1°C to over 10°C, depending on factors such as city size, surface cover type, and meteorological conditions. For instance, in large cities like New York and New Jersey, surface temperatures have shown a slow upward trend over the past two decades due to concentrated urban development, significantly impacting residents' quality of life in SUHI zones (Yin et al., 2023). In the hill city of Ranchi, a temperature difference of 1.6°C between SUHI zones and rural areas was recorded (Das et al., 2024). These SUHI cores shift and expand over time and in response to environmental conditions, as observed in Beijing, where they have moved eastward in recent years (Yuan et al., 2024). In Isfahan, seasonal SUHI variations have been documented, with peak intensity occurring in winter (Montazeri and Masoodian, 2024).

SUHI affects biological, economic, and meteorological processes. It can lead to earlier plant blooming, extended growing seasons, and altered bird migration patterns. More critically, SUHI contributes to reduced air quality, increased prevalence of respiratory and cardiovascular diseases, and elevated heat-related mortality (Gosling et al., 2008; Tan et al., 2010). Additionally, SUHI alters local weather by modifying wind patterns, enhancing cloud formation, and influencing precipitation (Kaviani, 2001). Land use changes and vegetation loss play a significant role in SUHI expansion and intensification. In Tehran, districts 9, 13, 18, and 21 and especially district 22, which contains the most barren land record the highest surface temperatures compared to surrounding areas (Ghanbari et al., 2023). A negative correlation between surface temperature and the Normalized Difference Vegetation Index (NDVI) has also been observed (Shang et al., 2023).

In Shiraz, SUHI has intensified due to vegetation decline, uncontrolled urban sprawl, and the presence of barren lands. These changes have led to several adverse outcomes, including: Elevated surface temperatures (Industrial zones and high-traffic streets experience extreme heat), Declining air quality (Higher temperatures exacerbate pollution and particulate matter), Increased energy consumption (Greater cooling demands strain electricity resources), Health risks (Vulnerable populations face heightened exposure to heat-related illnesses), Urban inequality (Low-income neighborhoods are more susceptible due to weak infrastructure and limited green space), Environmental disruption (Urban expansion threatens habitats and biodiversity) (Halabian and Soltani, 2020; Mohammadi and Afifi, 2021).

Given Shiraz's status as a major metropolis in southern Iran, several studies have explored various aspects of SUHI. Mobaraki (2012) emphasized population density, building concentration, and industrial activity as primary drivers. Sarbaz Demiri (2019) and Mohammadi and Afifi (2021) highlighted the role of land use change and industrial zones in SUHI intensification. Ziari et al. (2025) and Shoja et al. (2025) focused on evaluating the Heat Mitigation Index (HMI) and the extent of SUHI reduction across Shiraz, underscoring the importance of green infrastructure and environmentally responsive design.

This study aims to identify urban areas in Shiraz that are most affected by the Surface Urban Heat Island (SUHI) phenomenon, separately during daytime and nighttime. Additionally, it seeks to detect regions whose SUHI conditions have either intensified or mitigated over the study period due to environmental variations. Based on these findings, urban planners, environmental agencies, and policymakers will be able to formulate effective strategies to reduce SUHI impacts and enhance urban resilience in Shiraz.

2. Material and methods

2.1. Study site

The population of Shiraz was 1,725,221 according to the 2023 census, making it the fourth largest and most populous city in Iran and the most populous city in the south of the country. In the same year, 582,257 households lived in the city. The city is located at an altitude of 1,484 meters above sea level in the Zagros mountainous region and has a temperate climate (Table 1). Shiraz is bordered by Mount Drak to the west and by the Bemo, Sabzpushan, Chehel Maqam, and Babakouhi mountains (of the Zagros Mountain range) to the north, and it extends from north to southeast following the general direction of the Zagros Mountain range. The Shiraz plain is located between these heights. A seasonal river passes through the middle of the city, known as the Khoshk River, and has water only in winter and spring (Fig. 1). This river flows into Maharlu Lake in the

southeast of Shiraz. The city of Shiraz is divided into 11 municipal districts and has an area of over 217 square kilometers (Shiraz city annual report 2022-2023, 2024).

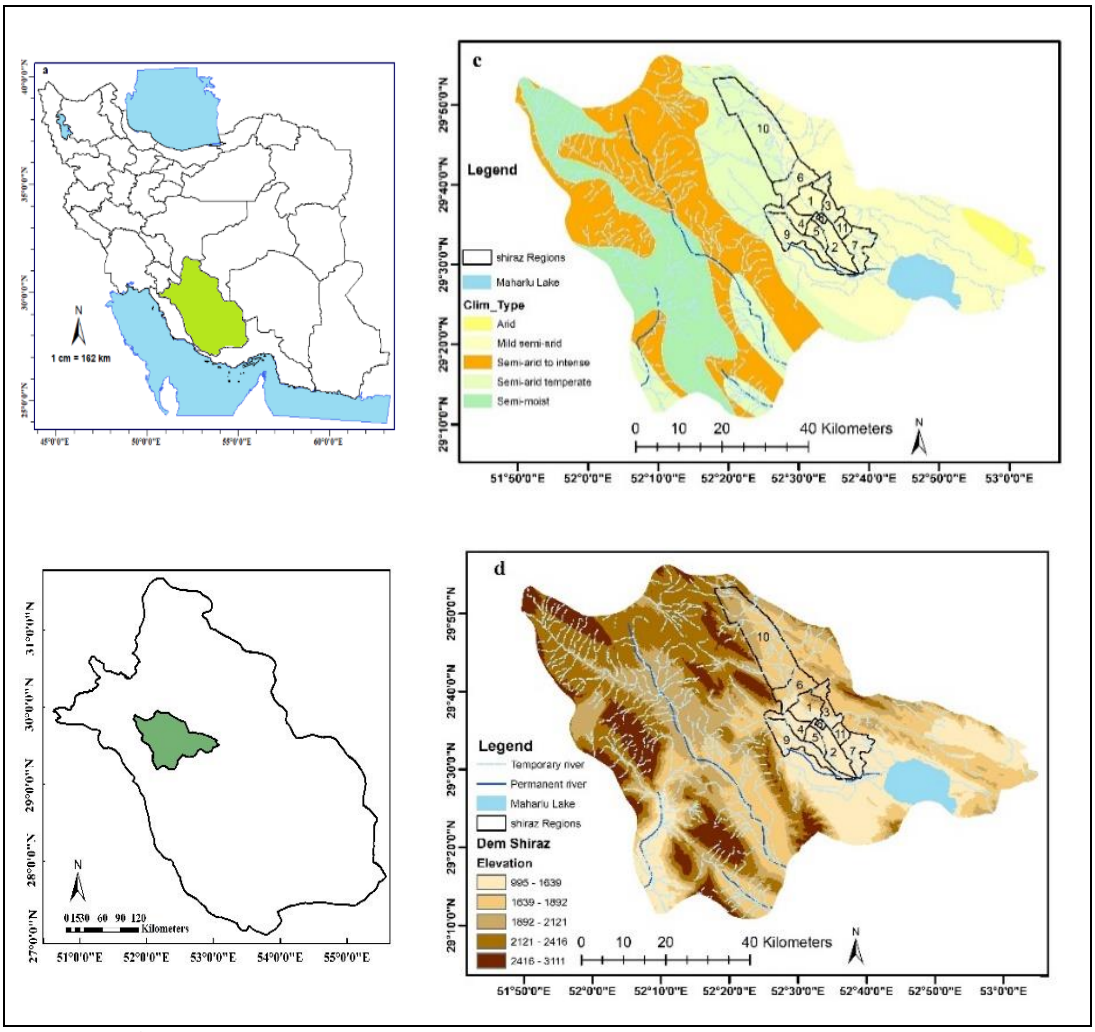


Fig. 1. The Map of the geographical location, a: Fars Province in Iran, b: Township Shiraz in Fars province, c: Climatological Shiraz township & city, d: Topography Shiraz township & city.

Table 1. Average climatic conditions of Shiraz city (1971-2025).

City	Latitude	Longitude	Elevation (m)	Mean Precipitation (mm)	Mean Min Temperature (°C)	Mean Max Temperature (°C)	Mean Relative Humidity (%)
Shiraz	52.36	29.32	1488	314	10.4	26	40

2.2. Data

Three categories of data were used in this study. First, LST data from the MODIS sensor installed on two Terra/ Aqua satellites was utilized. The MODIS sensor installed on these satellites has many products with different temporal and spatial resolution capabilities. The Terra satellite passes over Iran once between 10:00 to 12:00 LST during daytime and once between 21:00 to 23:30 LT during nighttime. Among various temperature products of MODIS, the MOD11A2 was selected because it had the proper technical specifications for the period from January 1, 2000, to December 31, 2024. Both night and day data were obtained. The projection system of this product is the sinusoidal equivalent. The provided data are in the form of tiles with 10 geographical degrees (1200 × 1200 pixels) in HDF format and with a resolution of approximately 1000 m. The MODIS LST is derived from two thermal infrared bands (TIR) operating at 10.78–11.28 μm and 11.77–12.27 μm wavelengths. The emissivity values from these two bands are converted to LST (in K) using the algorithm given below (Eqs1-3):

$$T_s = C + \left(A_1 + A_2\frac{1-\varepsilon}{\varepsilon} + A_3\frac{\Delta\varepsilon}{\varepsilon^2}\right)\frac{T_{31}+T_{32}}{2} + \left(\left(B_1 + B_2\frac{1-\varepsilon}{\varepsilon} + B_3\frac{\Delta\varepsilon}{\varepsilon^2}\right)\frac{T_{31}+T_{32}}{2}\right) \quad (1)$$

$$\varepsilon = (\varepsilon_{31} + \varepsilon_{32})/2 \quad (2)$$

$$\Delta\varepsilon = \varepsilon_{31} - \varepsilon_{32} \quad (3)$$

where Ts = LST, T31 and T32 are MODIS band 31 and 32 brightness temperatures; ε31 and ε32 are MODIS band 31 and 32 surface emissivity; C, A1, A2, A3, B1, B2, and B3 are regression coefficients (Eq. 4).

$$T_s(k) = a_0(k) + a_1(k)T_{11} + a_2(k)T_{12} + a_3(k)(T_{11} - T_{12})^2 + a_4(k)(\sec\theta - 1) \quad (4)$$

Where k is the index of the surface types and θ is the satellite viewing angle.

LST = (LST image in kelvin*0.02)-273.15 (5)

MODIS provides satellite imaging capabilities during the day and night. Its thermal bands are used to produce images of land surface temperatures (LST) (Eq. 5). LST data at night are more accurate than daytime data because they are free of the effects of daily solar radiation and allow for more accurate temperature estimates. Therefore, nighttime thermal data provides more accurate monitoring of the urban heat island. MODIS sensor products are available daily and 8-day with a spatial resolution of 1×1 km. The advantage of 8-day composite data in a time interval is that there is not much cloud in this data compared to daily data, and with the least amount of loss of each frame, the time series of its changes can be obtained. However, in daily data, there may be no data that causes errors. In this study, due to the length of the statistical period, most of the Terra satellite data in the period from January 1, 2000, to December 31, 2024 from the Earth Engine site and in the form of 8-day composite data were used. 1143 images were retrieved. The second series of data was land cover. In this study, the MODIS/Terra and Aqua Combined Land Cover product (MCD12Q1) was employed to classify land cover types across the study area. This dataset integrates reflectance data from both Terra and Aqua satellites, utilizing spectrally corrected inputs derived from the MODIS Nadir Bidirectional Reflectance Distribution Function Adjusted Reflectance (NBAR) product. Specifically, reflectance values from the red, near-infrared (NIR), shortwave infrared (SWIR), and blue bands were used to enhance classification accuracy. Land cover classification was performed using a supervised decision tree algorithm, which assigns land cover types based on spectral signatures and ancillary data. The product provides multiple classification schemes, including the International Geosphere-Biosphere Programme (IGBP), the University of Maryland (UMD), and the LAI/FPAR scheme. For this research, the IGBP classification was selected due to its comprehensive categorization of 17 land cover classes, encompassing natural vegetation types, urban areas, croplands, and barren lands. This dataset offers annual global coverage at a spatial resolution of 500 meters, making it suitable for regional-scale land cover analysis and change detection (Wang et al., 2007). For this data, images from 2002, 2012, and 2022 in HDF format were used. The third data series, land surface data includes variables such as the percentage of greenspace coverage, public greenspace area (m²), relative population density (per hectare), population (per hectare), area (hectares), number of households, and building permits across 11 municipal districts. This information was sourced from the 2024 Annual Report of Shiraz Municipality. Additionally, minimum and maximum temperature data for the years 1971 to 2024 were obtained from the National Meteorological Organization.

2.3. Method (Identifying UHIs and calculating their changes and intensity)

Among the studies conducted in recent years, those that utilize multi-temporal thermal imagery are of particular importance. Such studies allow for the investigation of both spatial and temporal variations in urban heat islands. To analyze these changes, some researchers employ classical statistical methods. However, due to the seasonal and monthly fluctuations in thermal imagery, directly comparing absolute temperature values is not appropriate. To enable meaningful comparisons, the thermal data must first be standardized. Researchers typically use one of two approaches for this: mean and standard deviation, or Minimum and maximum temperature values of each image. In this study, the data were standardized using the mean, and linear regression was applied to assess the

trends. To prepare the LST data, a function was defined to retrieve both daytime and nighttime temperature values. The average LST for daytime (LST_Day) and nighttime (LST_Night) was then calculated using a scale factor of 0.02, applied uniformly across all data spanning the past 25 years. The results were visualized using a color palette of blue, white, yellow, and red within a specified temperature range. In daytime imagery, the temperature difference between urban areas and their surroundings is minimal due to the influence of solar radiation. This additional heating masks the contrast between urban heat islands (UHIs) and other regions, making it difficult to observe and distinguish them. For arid and semi-arid regions, nighttime temperature data is more suitable for detecting UHIs. The ee.Reducer.linearFit function is one of the powerful tools in Google Earth Engine for temporal trend analysis, and it can be effectively used to detect urban heat island (UHI) changes. Using this function, we can examine whether the land surface temperature (LST) in a particular region is increasing or decreasing over time. This is done by calculating the slope of temperature changes across the time series (Fig. 2). The analysis steps are as follows: **collect land surface temperature** (LST) data(was use satellite imagery), **add a time band to the images**, **apply linearFit** function for calculates the trend, **interpret the output** (the scale band indicates the rate of temperature change, positive value: temperature is increasing (a sign of expanding heat islands), negative value: temperature is decreasing), **the offset band indicates the initial temperature value**(by displaying the scale band on the map, can identify areas where temperature is increasing (shown in red). These areas are usually the UHIs that are expanding.

LST changes are obtained through a linear regression of LST-Night values over a time series, reflecting the intensity of temperature variation.

Higher numerical values indicate more significant changes.

- Positive values represent an upward trend in LST,
- Negative values indicate a downward trend.

This analysis allows us to visualize thermal anomalies across the past 25 years.

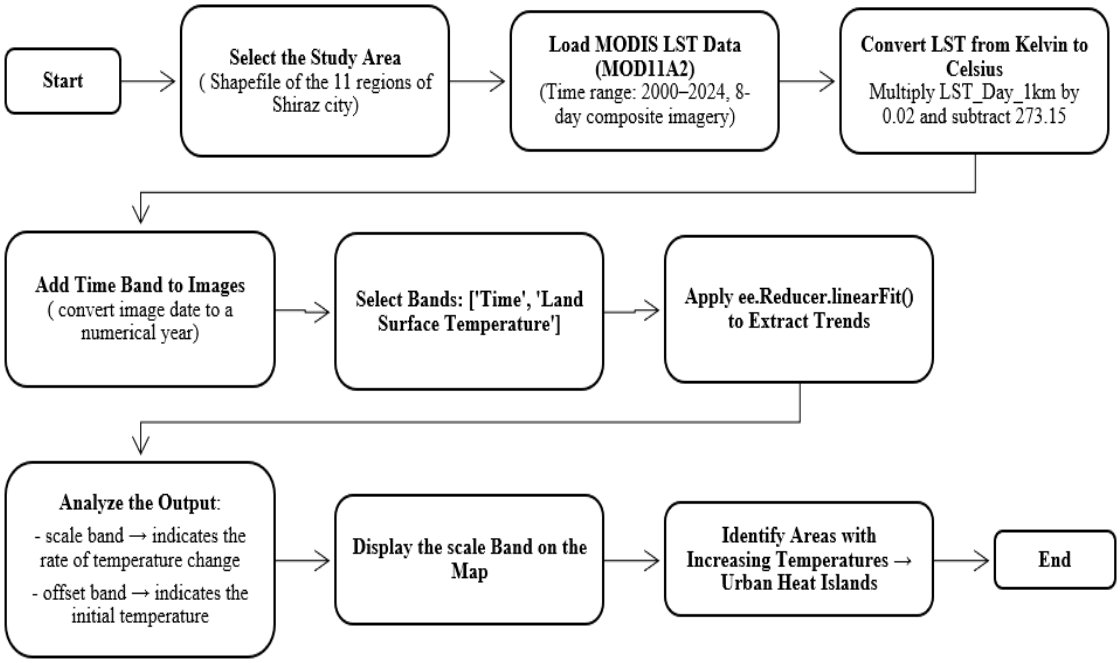


Fig. 2. The Flowchart showing the process of UHI trend estimation with ee.Reducer.linearFit.

2.4. Urban thermal behavior and spatial LST profiles

During the morning hours, the Surface Urban Heat Island (SUHI) exhibits significant amplitude and spatial variability, particularly in densely urbanized zones. Interestingly, Urban Heat Island (UHI) effects may show lower surface temperatures in built-up areas compared to vegetated zones during this period.

This counterintuitive pattern arises due to the thermal inertia of urban materials and the mass per unit area required for heating areas with fewer horizontal and vertical constructions tend to warm up more quickly.

Moreover, the thermal properties of surface materials, their spatial arrangement, and architectural geometry play a crucial role in modulating heat exchange. Shading effects from buildings and the heterogeneity of urban surfaces (e.g., concrete, asphalt, glass) contribute to a complex heating and cooling dynamic, making urban thermal behavior highly variable across space. The spatial profile of Land Surface Temperature (LST) further illustrates this complexity. LST maps often reveal sharp gradients between built-up and vegetated areas, with hotspots forming in regions with low vegetation cover, high impervious surface fraction, and reduced Sky View Factor (SVF). SVF, which quantifies the openness of the sky from a given point, is lower in urban canyons, leading to reduced radiative cooling and greater heat retention, especially at night. Around midday, SUHI intensifies due to peak solar radiation and the cumulative heating of urban surfaces. At night, urban areas retain more heat than their rural counterparts, driven by the thermal behavior of construction materials, surface albedo, and limited exposure to the sky, which inhibits longwave radiation loss.Understanding the spatial LST profile is essential for urban climate studies, as it helps identify critical zones for heat mitigation strategies, such as increasing green cover, optimizing building materials, and improving urban geometry to enhance SVF and airflow.Another effective approach for identifying and spatially delineating Urban Heat Islands (UHI), as well as assessing temperature differences between urban and suburban areas, involves analyzing temperature profiles across the city. This method can be implemented using Land Surface Temperature (LST) data derived from MODIS satellite imagery (Hughes et al., 2012; Ahrari, 2020). To apply this technique, a transect line was drawn across the city in a northwest–southeast direction (Fig. 3). The average LST values along this line were extracted and analyzed for both daytime and nighttime periods. This allowed for a detailed examination of spatial temperature variations and the intensity of the UHI effect across different urban zones. Peaks in the profile typically correspond to urban cores, while troughs indicate cooler suburban or vegetated zones. The difference between day and night profiles helps assess the persistence and intensity of UHI.

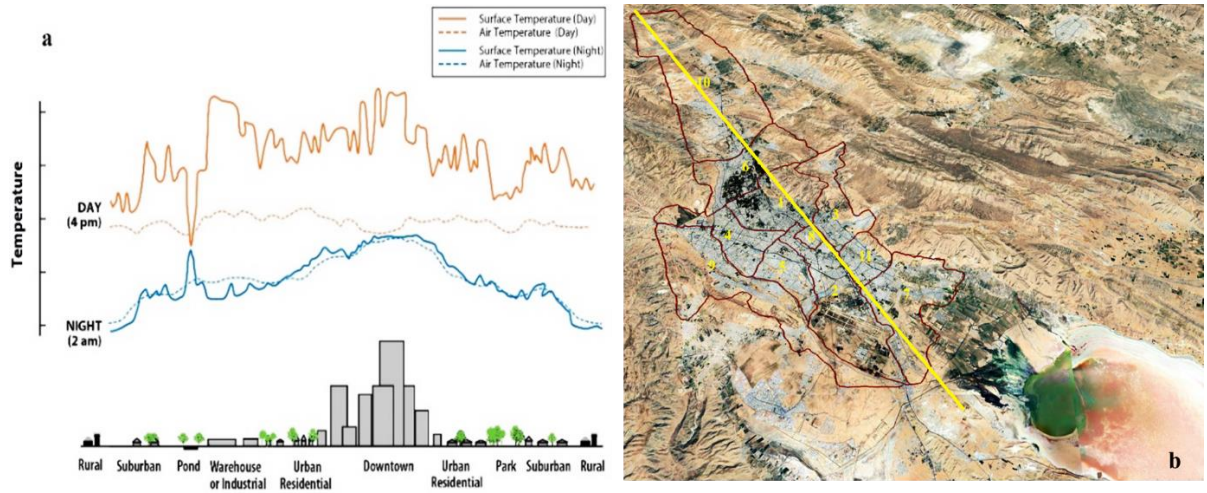


Fig. 3. The temperature profile in different areas, with the formation of the SUHI (a), Spatial LST Profile in Shiraz metropolitan (b), Sources: Usage: Public Domain, Author's (b).

The distribution of urban heat islands in Shiraz has been explored in numerous studies; however, this research differs from previous ones in several key ways:

=Use of Updated Data and Detailed Urban Area Analysis: Unlike earlier studies that relied on outdated maps, statistics, and information, this research employs modern maps of Shiraz's urban zones and conducts a separate analysis of all 11 districts. This method aims to pinpoint the most vulnerable areas, laying the

groundwork for future research and strategic urban planning by municipal authorities.

=Comprehensive Temporal Coverage Over 25 Years: This study spans a full 25-year period (from January 1, 2000, to December 31, 2024), analyzed in 8-day average intervals. In contrast, most previous research was based on limited satellite data collected on specific individual days.

=Trend and Intensity Assessment Using Linear Regression and LST Standard Deviation: By applying linear regression to time-series data and nighttime land surface temperature (LST), this study evaluates the trends and intensity of urban heat island changes-highlighting the districts that have undergone the most significant transformations and impacts over the past 25 years. This analytical approach has not been used in earlier studies.

3. Results and discussion

The area of Shiraz City expanded from 179 square kilometers and 9 urban districts in 2006 to 217 square kilometers and 11 districts by 2016, and this remained unchanged through 2024.However, the city's population grew from 1,351,181 to 1,725,221 during this period. According to Table 2 and Fig.4(b), the highest population densities are observed in districts 4, 5, and 3. Shiraz has a hot, semi-arid climate, with prevailing winds from the west and northwest (Fig.1). Urban green spaces—an important factor in mitigating urban heat islands—are primarily concentrated in districts 4, 5, 2, and 11, as illustrated in Table 2 and Fig. 4(a).

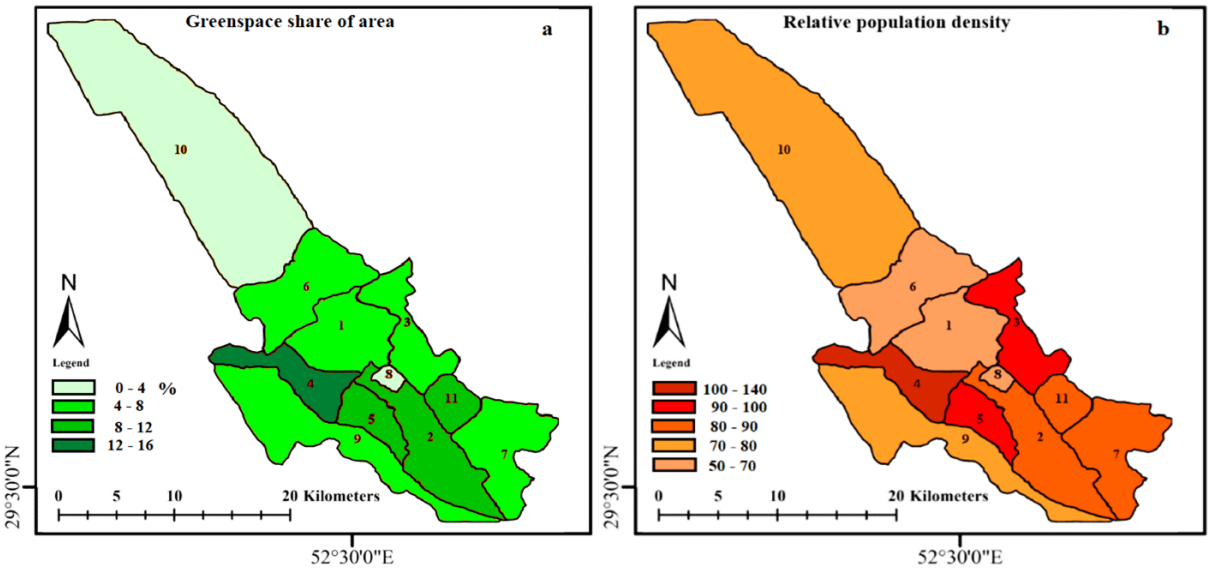


Fig. 4. The map of Greenspace shares of area %(a) & Relative population density per HA(b).

Table 2. Estimation of population and green space indices by municipal regions of Shiraz city in 2024.

Regions	Area (HA)	Population (Per HA)	Relative population per HA density	Public Greenspace Area m^2	Greenspace share of area %
1	2556	145195	56.8	1555448	6.09
2	1800	151539	84.2	1049268	**8.83**
3	1447	135672	**93.8**	961800	6.65
4	2354	313568	**133.2**	3193743	**13.57**
5	1680	160391	**95.5**	1503074	**8.95**
6	2426	125318	51.7	1650394	6.8
7	1716	144801	84.4	1129800	6.58
8	368	20506	55.7	141431	3.84
9	2943	212886	72.3	1391093	4.73
10	3187	214414	67.3	1219885	3.83
11	1214	100931	83.1	1068369	**8.8**

Source: Shiraz city annual report 2022-2023, 2024.

A linear regression analysis of temperature trends over the past 54 years reveals a 2.16°C rise in the average annual maximum temperature and a 1.57°C increase in the average annual minimum temperature (Fig. 5). The most significant rise in minimum temperatures has occurred during autumn and spring, while the greatest increase in daily temperatures has been observed in winter and spring (Table 3). These findings suggest that the climate of Shiraz is being influenced by global warming. Considering this trend, along with growing population pressure and land use changes in and around Shiraz, the need to address and study urban heat islands as a major environmental challenge becomes increasingly important.

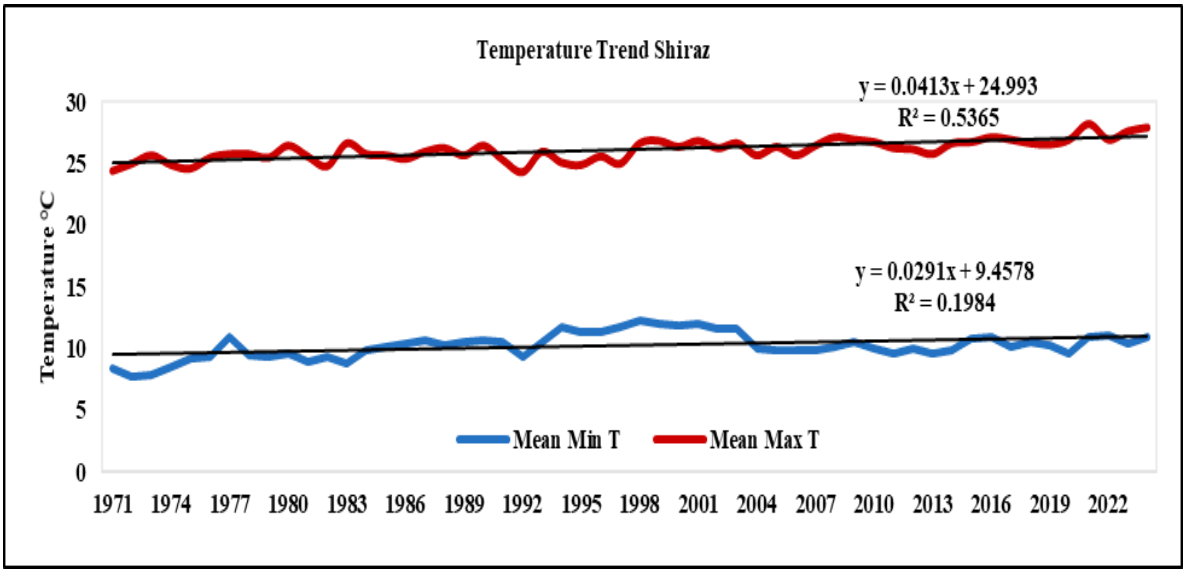


Fig. 5. Trend annual mean min and max temperature in Shiraz.

Table 3. Estimation Monthly changes in temperature in Shiraz.

Month	Season	T min	p-value	Variation	T Max	p-value	Variation
Jan	Winter	y = 0.0139x - 0.056	0.0000063	+0.74	y = 0.0559x + 11.528	<0.0001	+2.96
Feb		y = 0.0258x + 0.4427	0.0000079	+1.37	y = 0.0561x + 12.447	<0.0001	+2.97
Mar		y = 0.0229x + 3.8073	0.0000092	+1.21	y = 0.0772x + 16.123	<0.0001	+4.1
Apr	Spring	y = 0.0261x + 7.4058	0.0000002	+1.39	y = 0.053x + 21.189	<0.0001	+2.8
May		y = 0.0296x + 12.048	0.0000001	+1.57	y = 0.0344x + 28.091	<0.0001	+1.8
Jun		y = 0.0354x + 16.36	0.0000003	+1.9	y = 0.0341x + 34.492	<0.0001	+1.8
Jul	Summer	y = 0.0335x + 19.698	0.0000005	+1.78	y = 0.0302x + 37.553	<0.0001	+1.6
Aug		y = 0.0306x + 19.813	0.0000009	+1.6	y = 0.025x + 37.201	<0.0001	+1.3
Sep		y = 0.0385x + 15.921	0.0000012	+2	y = 0.0222x + 34.705	<0.0001	+1.2
Oct	Autumn	y = 0.046x + 10.5	0.0000021	+2.4	y = 0.041x + 29.005	<0.0001	+2.1
Nov		y = 0.0399x + 5.3412	0.0000035	+2.1	y = 0.0152x + 22.344	<0.0001	+0.8
Dec		y = 0.0174x + 1.7654	0.0000048	+0.9	y = 0.0101x + 16.005	<0.0001	+0.5
Annual		y = 0.0292x + 9.4565	0.0000004	+1.5	y = 0.0413x + 24.993	0.0000001	+2.1

To better compare and understand changes in land cover, maps from the years 2002, 2012, and 2022 prepared using MODIS satellite imagery were analyzed. Land cover within the Shiraz metropolitan area is generally classified into five categories: Grasslands, Croplands, Shrub lands, Urban and Built-up areas, and Barren or Sparsely Vegetated lands. Among these, Shrub lands and Urban and Built-up areas constitute the largest share of land use. In contrast, Barren or Sparsely Vegetated areas account for the smallest proportion (Fig. 6 and Table 4). A review of land cover maps in recent years shows that urban construction has not expanded significantly, but the amount of pasture and agricultural land has decreased, and

the amount of Shrub lands and wasteland has increased in the urban area of Shiraz. A comparison of land use maps over the three years 2002, 2012, and 2022 shows that most of the decrease in agricultural land has occurred in the southern areas of the city, and the northern half, we are witnessing more of an increase in the expansion of wasteland and pastures (Fig .6 and Table 4).

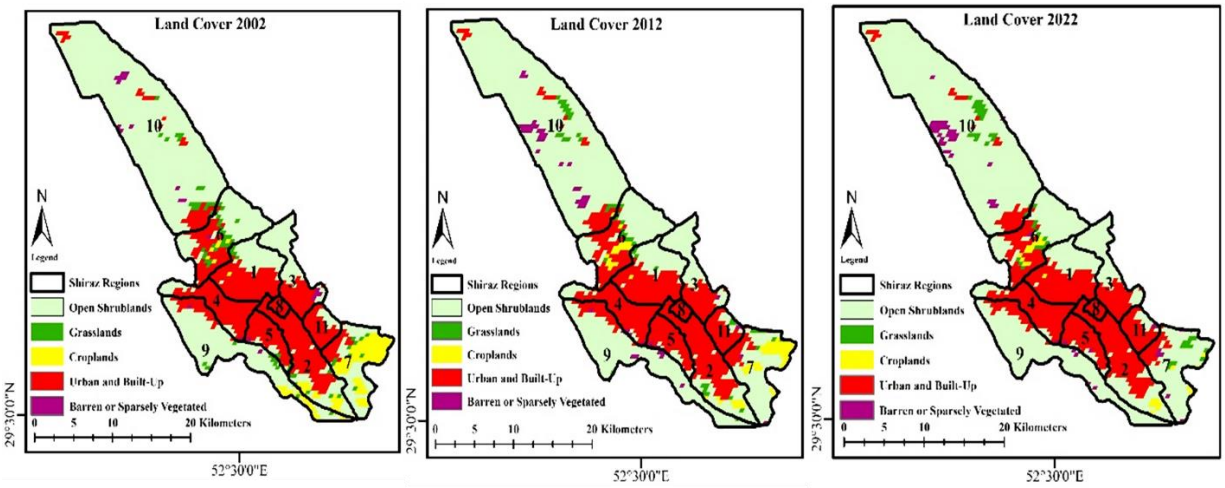


Fig 6. Land cover change in Shiraz metropolitan at 2002,2012 and 2020.

Table 4. Land cover change in Shiraz metropolitan at 2002,2012 and 2020.

Land cover/Year	2002		2012		2022	
	Area ($Km^{2)}$	Area (%)	Area ($Km^{2)}$	Area (%)	Area ($Km^{2)}$	Area (%)
Shrub lands	132	60.8	138	63.6	142.4	65.6
Grasslands	7.4	3.5	4.8	2.2	4.4	2
Croplands	12.2	5.6	6.1	2.8	2.3	1.1
Urban and Built-up	63.6	29.3	63.6	29.3	63.6	29.3
Barren or Sparsely Vegetated	1.8	0.8	4.5	2.1	4.3	2

To investigate the spatial pattern of urban heat islands in the Shiraz metropolitan area, maps of mean Land Surface Temperature (LST) during both day and night, along with nighttime temperature changes over the past 25 years, were analyzed. In these maps, blue and white areas indicate cooler regions, while red and yellow areas represent warmer regions typically associated with heat islands. According to the results shown in Fig. 7, daytime heat islands appear as scattered clusters, mainly concentrated in the southern and northeastern parts of the city. During the day, the temperature difference between heat island cores and cooler urban regions reaches approximately 3°C. Most of the cooler areas are located in the city center, particularly regions 1 and 6, which benefit from higher elevation, proximity to mountain slopes, lower building density, widespread urban gardens, and open spaces that facilitate air ventilation. In contrast, regions 2, 7, and 9 are identified as daytime heat islands. This phenomenon is not only due to increased construction activity but also stems from the conversion of agricultural lands into barren plots, which reduces surface moisture and evaporation, thereby increasing surface temperatures. Additionally, the presence of Shahid Dastgheib International Airport and an industrial park in these zones further intensifies the heat island effect. Given Shiraz's semi-arid climate, nighttime LST maps were generated to eliminate the influence of solar radiation and enhance the visibility of heat islands. As shown in Fig. 7, nighttime heat islands are primarily concentrated in central urban areas, which are characterized by high building density, limited green space, and aging urban fabric especially, in region 8, the historical core of the city. These areas suffer from inadequate natural ventilation due to dense construction and a lack of open space.

Conversely, the coolest nighttime zones are found in region 10, located in the northern part

of Shiraz, where higher elevation contributes to lower surface temperatures. At night, the temperature difference between cold cores and urban heat islands reaches up to 3.5°C. To assess long-term temperature trends, a standard deviation map of nighttime LST was also produced. In this map:

- Positive values indicate an upward trend in surface temperature,
- Negative values reflect a declining trend over time.

Overall, urban expansion and the development of new residential areas have predominantly occurred in red-marked regions experiencing rising temperatures. As illustrated in Fig. 7, the most significant changes in surface temperature over the past 25 years have taken place in the northern half of Shiraz, where land use transformation, construction activity, and population growth have been most pronounced. In zone 10, lower land and rental prices have attracted more residents in recent years. Meanwhile, the emergence of heat islands in zone 6 is primarily due to the conversion of Qasr al Dasht gardens into residential land and the resulting increase in building density. Notably, rising temperature patterns are observed in districts 4, 10, 6, 1, and the northern portion of district 7, where extensive development has taken place in recent years especially in districts 10 and 7. In district 1, the increase in LST is attributed not only to new construction but also to the loss of traditional garden areas, which previously moderated surface temperatures.

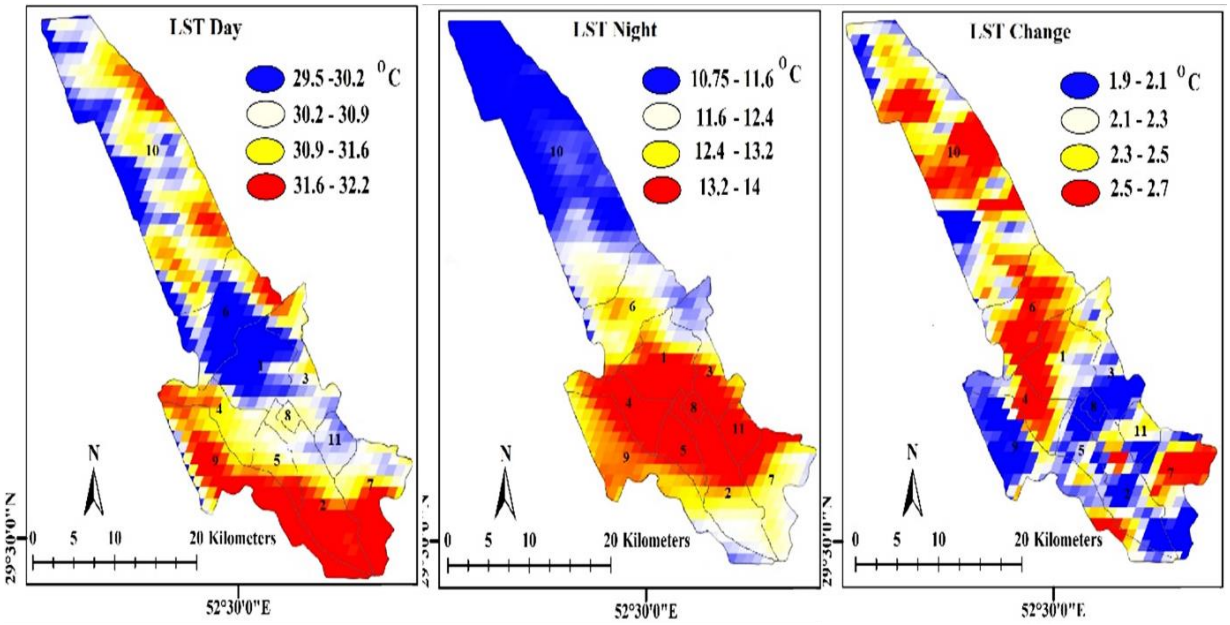


Fig. 7. Day and night LST map and night LST changes over the last 25 years in Shiraz metropolitan.

To enhance the accuracy of the analysis, annual nighttime LST values were extracted for four urban districts 4, 10, 1, and 6 where temperature fluctuations were more pronounced. As depicted in Fig. 8, temperature peaks across these districts occurred in the years 2000, 2010, 2016, 2018, and 2021. These temperature peaks in the LST_Night time series align with the peak values observed in the annual time series of average minimum and maximum temperatures recorded at the Shiraz meteorological station (Fig. 5), indicating a consistent warming trend across the entire city. Among the selected districts, regions 4 and 1 consistently exhibited higher temperatures, while region 10 remained cooler. The relatively lower temperatures in region 10 are attributed to the presence of extensive garden areas and their elevated topography, which naturally moderates surface heating. In contrast, the elevated LST levels in regions 4 and 1 are primarily linked to higher population density and a surge in construction activity, both of which contribute significantly to urban heat intensification.

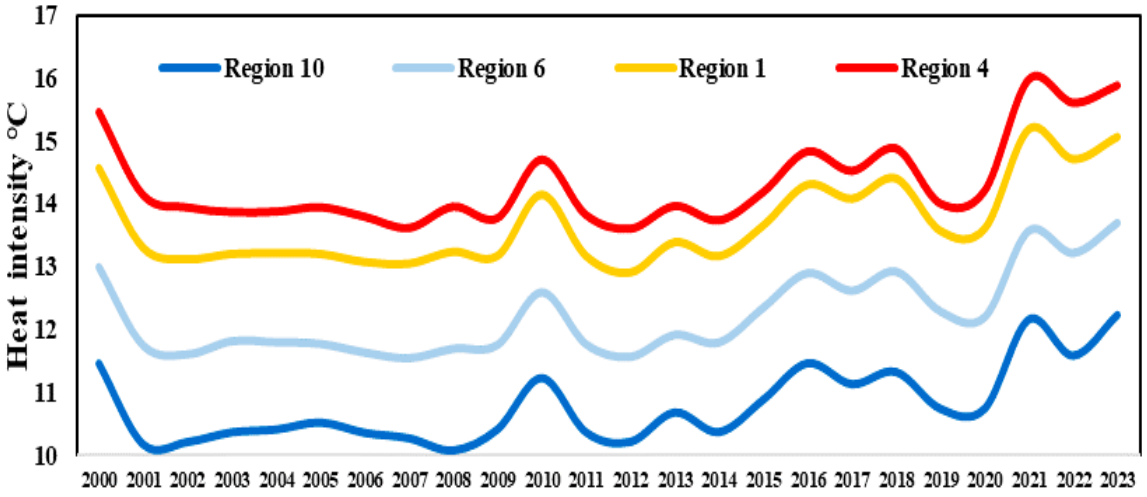


Fig. 8. Surface SUHI intensity index in the 4 districts Shiraz metropolitan area based on LST_Night.

In region 7, alongside population growth and increased construction activity, rising temperatures are further influenced by the proximity of the Shiraz municipal landfill located in the Barmashor area, which spans approximately 5,000 hectares. Municipal solid waste deposited in the landfill undergoes a biochemical process known as biodegradation, resulting in the production of landfill gas. This gas, a byproduct of decomposing biodegradable waste, contains 40 to 60 percent methane along with varying concentrations of other gases (Rezaee and Abolhasani, 2018). As a potent greenhouse gas, methane plays a critical role in atmospheric warming and subsequently elevates surface temperatures. Region 4, identified as the warmest among Shiraz's 11 urban districts, was selected for in-depth analysis due to its stable boundaries and area over the past 18 years. To assess the impact of construction growth, the issuance of building permits across different districts was examined. Throughout the study period, region 4 consistently ranked second in the number of housing construction permits issued except in 2012, when Regions 1 and 6 led, and from 2019 onward, when region 7 emerged among the top-ranking districts. In addition to building permits, data on area size, total population, and relative density per hectare were analyzed. Up until 2015, relative density increased gradually, but after 2016, there was a notable surge in both population and density indicators. Given that only 0.73% of region 4 comprises dilapidated structures, the growth in population and construction activity suggests a trend toward higher building density, mass housing development, and vertical expansion through high-rise construction (Table 5).

Table 5. Population and area indicators and issuance of building permits in District 4 of Shiraz Municipality.

Year	Aria HA	Population	Number of households	Relative population density per HA	Number of Building Permit	Ratio of Building Permit by Region 4 to Shiraz %
2006	2,318	196,320	50,819	85	808	31
2007	2,318	196,320	50,819	85	833	24.9
2008	2,318	196,320	50,819	85	551	16.5
2009	2,318	196,320	50,819	85	589	14.56
2010	2,318	196,320	50,819	85	568	19
2011	2,318	196,320	50,819	85	829	16
2012	2,318	226,412	66,396	98	944	16
2013	2,866	266,970	78,287	93	956	13
2014	2,866	237,906	69,770	83	452	14
2015	2,866	241,351	70,780	84	482	13
2016	2,354	243,617	71,372	103	402	13
2017	2,354	258,058	81,558	110	455	10

Year	Aria HA	Population	Number of households	Relative population density per HA	Number of Building Permit	Ratio of Building Permit by Region 4 to Shiraz %
2018	2,354	261,663	82,698	111	201	9.5
2019	2,354	265,317	88,700	113	367	10.4
2020	2,354	287,956	96,517	122	396	10.7
2021	2,354	296,450	96,517	126	505	12
2022	2,354	304,989	105,243	130	500	12
2023	2,354	313,568	109,781	133	505	14.2

Source: Shiraz city annual report 2022-2023, 2024.

Day–Night Thermal Variation Across the Urban Transect: Based on the transect line illustrated in Fig. 3, which was drawn across the city center, Land Surface Temperature values were calculated along this axis to assess spatial variations in surface temperature across different urban zones. As illustrated in Fig.=9, during the daytime, the city center exhibits lower surface temperatures compared to the surrounding outskirts. The minimum daytime LST is 28.4°C, while the maximum reaches 34.6°C, indicating a temperature difference of 6.2°C. In contrast, nighttime conditions reveal an opposite trend. As one moves toward the historical core and central urban areas, surface temperatures increase. The minimum average nighttime LST is 10.7°C, and the maximum is 15.4°C, resulting in a temperature difference of 4.7°C (Fig. 9)=

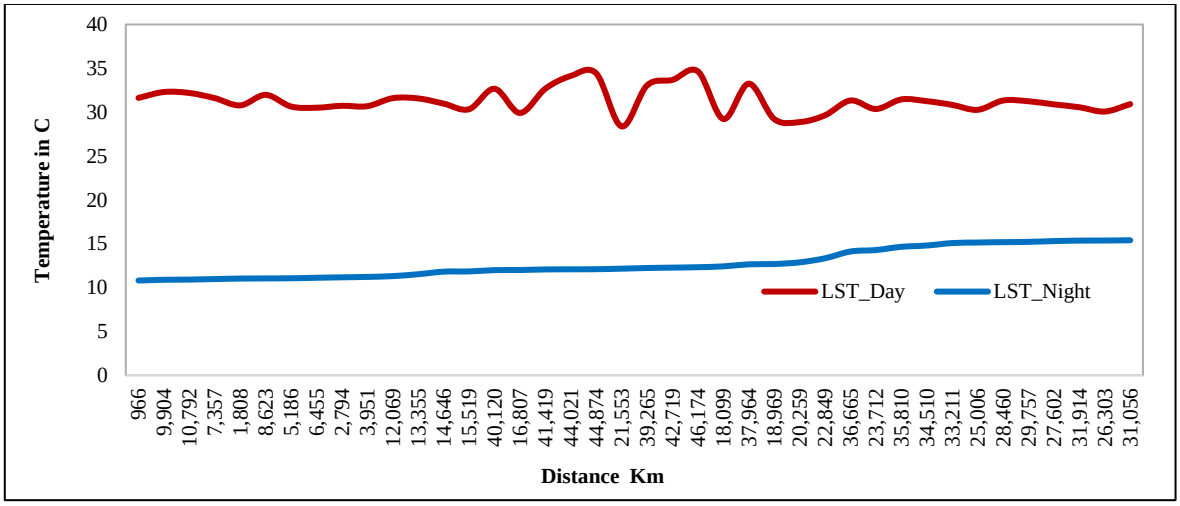


Fig. 9. LST change at day and night along in Shiraz metropolitan.

In recent years, the phenomenon of Urban Heat Islands (SUHI) has become increasingly prevalent in metropolitan areas like Shiraz. This is largely due to the combined effects of global warming, rapid population growth, urban expansion, and changes in land cover. As cities grow, natural surfaces are replaced with impervious materials such as concrete and asphalt, which absorb and retain heat, leading to significantly higher temperatures in urban cores compared to surrounding rural areas (Mobaraki, 2012; Shoja et al., 2025). According to studies, the temperature difference between urban and suburban areas in Shiraz can reach up to 2.98°C, with the most intense heat observed in densely built districts (Shoja et al., 2025). This temperature disparity increases the demand for air conditioning and energy consumption, exacerbating environmental and economic pressures (Shoja et al.2025; Ziari et al.2025). Recommended Mitigation Strategies for Shiraz: To address the SUHI effect and reduce the temperature gap between urban and suburban zones, the following urban planning and design strategies are proposed for implementation by city officials in Shiraz:

- Surface and Structural Design (Use of light-colored materials for buildings, streets, and sidewalks to increase albedo and reflect solar radiation (Shoja et al., 2025). Optimize building geometry to minimize direct sunlight penetration and reduce heat absorption (Mobaraki, 2012). Design wind-permeable street layouts to facilitate natural ventilation and enhance cooling effects (Mobaraki,2012).

- Green Infrastructure (Expand green spaces and urban parks, especially in high-density districts, to promote evapotranspiration and shading (Shoja et al.2025, Ziari et al.2025). Encourage green roofs and walls through incentives, as vegetation can reduce surface temperatures by up to 0.42°C (Mobaraki,2012). Integrate suitable plant species that thrive in Shiraz's climate to maximize cooling capacity (Shoja et al.2025). In arid cities spanning 150–200 km², vegetation contributes to cooling SSUHI by up to 61 %, but this effect lessens in larger cities (Deng et al., 2024). The municipality has actively pursued the acquisition of private gardens across the city most, notably the Qasr-al-Dasht gardens in Zone 1, to preserve them as urban green spaces. In 2020 and 2021 alone, 18 such gardens were officially acquired by the municipality. In recent years, efforts have also been made to restore several historic gardens, including the 11-hectare Iranian Garden in Zone 4. Additionally, the large-scale Kooh-e-Noor Forest Park, spanning 1,100 hectares in Zone 3, has been inaugurated and opened to the public, marking a significant step toward enhancing urban ecological infrastructure**.**
- Innovative Cooling Techniques (Deploy fog machines in strategic urban areas to increase humidity and promote evaporative cooling).
- Public Engagement and Policy (Educate citizens on the benefits of public transportation and sustainable urban living to reduce vehicular emissions and heat generation (Ziari et al.2025). Promote smart urban growth by regulating building density and minimizing excessive land sealing (Mobaraki, 2012). Increase municipal budget allocations for temperature mitigation projects and climate-resilient infrastructure (Ziari et al.2025).
-The Role and Participation of the Municipality and Urban Planning Authorities. Implementing an electric bus system and expanding metro lines in central urban areas, Developing dedicated bicycle lanes, Enforcing urban planning regulations and approved legal frameworks, especially the law governing land-use change of gardens and agricultural lands, Promoting urban agriculture in areas surrounding the airport and industrial zones, Implementing the law on relocating military garrisons outside the city boundaries (Heidari, 2024) and converting these sites into gardens and green spaces in Zones 1, 3, and 4, Revisiting high-rise construction regulations and avoiding dense development in heat island zones, while adhering to residential open space standards as outlined by the Supreme Council for Urban Planning and, Architecture (Heidari, 2024), particularly in the city center and Zones 1, 4, and 6, The slow and outdated public bus system has led to increased reliance on private vehicles, thereby exacerbating urban warming. Expanding dedicated bus lanes to improve transit speed could encourage greater public transport usage. Revitalizing deteriorated urban fabric around Zones 3 and 8 and increasing green space coverage in these areas, enhancing urban open spaces through approved redevelopment plans for historic and deteriorated districts, such as the 57-hectare Shahcheragh Shrine and Between-the-Shrines development project in Shiraz.

4. Conclusion

In recent years, rapid economic development has accelerated urbanization in Shiraz, leading to numerous environmental challenges. This study aims to investigate the Urban Heat Island (SUHI) phenomenon across different districts of Shiraz and to analyze its spatial and temporal dynamics. To achieve this goal, satellite-based remote sensing data from MODIS products and the Earth Engine platform were utilized. The findings reveal that the SUHI effect in Shiraz has intensified significantly, particularly during nighttime hours. By employing 8-day averaged Land Surface Temperature (LST) data over a 25-year period, the study enables a more precise assessment of temperature variations across the city. At night, the temperature difference between the city center and the suburbs reaches nearly 5°C. The results indicate that urban planning patterns, land use changes, and the spatial geometry of the urban fabric play a crucial role in the emergence and expansion of SUHI-affected zones. The dense and historic core of Shiraz, characterized by three-dimensional structures and vertical walls, traps solar radiation and restricts airflow, resulting in elevated nighttime temperatures. In the northern districts, the expansion of barren lands has contributed to increased daytime temperatures, while in the southern areas, the reduction of agricultural lands and the growth of built-up zones have led to higher nighttime temperatures. Considering the environmental and public health impacts of SUHI,

implementing management strategies such as expanding green spaces, preserving agricultural lands, and adopting climate-responsive architectural designs is essential. These measures can help mitigate thermal stress, improve urban quality of life, and promote sustainable development in the context of ongoing climate change.

Acknowledgments

This article was not under any financial support.

References

Ahrari, A., 2020, Satellite Image Processing Virtual Engine, Key to education, Tehran, p 219. https://girs.ir/product/gee-cookbook/

Das, B. K., Kush, A., & Pathak, A. (2024). Investigating Surface Urban Heat Island (SUHI) Effect for a Hill City. https://doi.org/10.21203/rs.3.rs-4296292/v1

Deng, X., Yu, W., Shi, J., Huang, Y., Li, D., He, X., Zhou, W. & Xie, Z., 2024. Characteristics of Surface Urban Heat Islands in Global Cities of Different Scales: Trends and Drivers. *Sustainable Cities and Society*, 107, 105483.

Ghanbari, R., Heidarimozaffar, M., Soltani, A. & Arefi, H., 2023. Land surface temperature analysis in densely populated zones from the perspective of spectral indices and urban morphology. *International Journal of Environmental Science and Technology*, 20(3), 2883-2902.

Gosling, S., Lowe, J., McGregor, G., Pelling, M. & Malamud, B., 2008. Associations between elevated atmospheric temperature and human mortality: a critical review of the literature. *Climatic Change*, 92(3-4), 299-341.

Halabian, A. & Soltani, Z., 2020. Analysis of spatial- temporal variation of urban thermal islands and landuse based on an environmental approach in Shiraz. *Urban Structure and Function Studies*, *7*(24), 73-97.

Heidari, A., 2024, Urban Planning Laws and Regulations. SAMT Publication. 142, 162p.

Hughes, C., Hook, S. J. & Hulley, G.C., 2012. MODIS MOD21 Land Surface Temperature and Emissivity Algorithm Theoretical Basis Document. *NASA Technical Publication*, 1347.

Imran, H.M., Shammas, M.I., Rahman, A., Jacobs, S.J., Ng, A. W.M. & Muthukumaran, S., 2021. Causes, modeling and mitigation of urban heat island: a review. *Earth Sciences*, 10(6), 244-264.

Kaviani, M.R., 2001, Microclimatology. SAMT Publication. 235p.

Mobaraki, A., 2012. Strategies for Mitigating Urban Heat Island Effects in Cities: Case of Shiraz City Center. Gazimağusa, North Cyprus M.Sc. Dissertation. Eastern Mediterranean University.

Mohammadi, M. & Afifi, M.E., 2021.Investigation of the occurrence of urban thermal islands phenomenon using ASTER satellite images (Study area: Shiraz city). *Journal of Geography and Environmental Studies*, 37(1), 21-44.

Montazeri, M. & Masoodian, S.A., 2024. Quantifying of surface urban heat island intensity in Isfahan metropolis using MODIS\Terra\LST data. *Atmósfera*, 38.

Rezaee, E. & Abolhasani, H., 2 018. Evaluation of Landfill Gas Generation for Exploitation Energy (Case Study: Landfill No. 2 of Shahinshahr). *Journal of Environmental Health Science & Engineering*, 5(4), 389-400.

Sarbaz Demiri, J., 2019. Studying the impact of urban green space on the temporal-spatial distribution of heat islands in Shiraz, Iran. M.Sc. Dissertation Mohaghegh Ardabil University.

Shang, K., Xu, L., Liu, X., Yin, Z., Liu, Z., Li, X. ... & Zheng, W., 2023. Study of urban heat island effect in Hangzhou metropolitan area based on SW-TES algorithm and image dichotomous model. *Sage Open*, 13(4), 21582440231208851.

Shiraz city annual report 2022-2023, 2024, Municipality Shiraz, 27.

Shoja, F., Roki, Z. & Shamsipour, A., 2025. Investigation of the impact of green infrastructure on reducing the urban heat load using the InVEST model: a case study of Shiraz city, Iran. *Theoretical and Applied Climatology*, 156(6), 311.

Sun, Q., Tan, J. & Xu, Y., 2010. An ERDAS image processing method for retrieving LST and describing urban heat evolution: a case study in the Pearl River Delta Region in South China. *Environmental Earth Sciences*, 59(5), 1047-1055.

Tan, J., Zheng, Y., Tang, X., Guo, C., Li, L., Song, G. ... & Chen, H., 2010. The urban heat island and its impact on heat waves and human health in Shanghai. *International Journal of Biometeorology*, 54(1), 75-84.

Vujovic, S., Haddad, B., Karaky, H., Sebaibi, N. & Boutouil, M., 2021. Urban heat island: Causes, consequences, and mitigation measures with emphasis on reflective and permeable pavements. *CivilEng*, 2(2), 459-484.

Yuan, D., Zhang, L., Fan, Y., Sun, W., Fan, D. & Zhao, X., 2024. Spatio-Temporal Analysis of Surface Urban Heat Island and Canopy Layer Heat Island in Beijing. Applied Sciences, 14(12), 5034.

Yin, Z., Liu, Z., Liu, X., Zheng, W. & Yin, L., 2023. Urban heat islands and their effects on thermal comfort in the US: New York and New Jersey. *Ecological Indicators*, 154, 110765.

Ziari, K., Golzar, M. & Iraji, H., 2025. Investigating the effects of urban green infrastructure on reducing the heat Island phenomenon in Shiraz metropolis. *Pollution*, 11(2), 394-410.